Journal of Organometallic Chemistry, 448 (1993) 139–149

JOM 23202

Synthesis and solution dynamics of $[Cp(CO)_2Fe]_2(CH{=}CH_2)^+BF_4^-$, a μ-($\eta^1:\eta^2$) vinyl complex not containing a metal–metal bond

D. Lawrence Tarazano, Thomas W. Bodnar and Alan R. Cutler

Department of Chemistry, Rensselaer Polytechnic Institute, Troy NY 12180 (USA)

(Received July 28, 1992; in revised form August 31, 1992)

Abstract

Treatment of $FpCH{=}CH_2$ with the Lewis acid precursor $Fp(THF)^+BF_4^-$ affords the stable, fully characterized $\mu(\eta^1:\eta^2)$ vinyl complex $(Fp{-}CH{=}CH_2)Fp^+BF_4^-$ (3) [$Fp = Fe(CO)_2(\eta^5\text{-}C_5H_5)$]. Its IR and ^1H, ^{13}C NMR spectral data are consistent with an unsymmetrical π-complex [as established for vinyl ether compounds $Fp(CH_2{=}CHOR)^+$] between $Fp{-}CH{=}CH_2$ and the second Fp group, in which positive charge is extensively delocalized over both iron centers. The spectroscopically distinct Fp centers interchange, although this μ-vinyl ligand oscillation is very slow on the NMR time scale at room temperature. Results of ^1H NMR magnetization transfer studies (using both spin saturation transfer and inversion transfer experimental procedures with the Cp resonances) converge on a first-order exchange rate constant $k_{AB} = 0.045\text{–}0.049\ s^{-1}$ at 25°C. The calculated $\Delta G^{\ddagger} = 19.3$ kcal/mol is 2–3 kcal/mol greater than the estimated minimum $\Delta G^{\ddagger}$ value for the known μ-vinyl compound $[Cp(CO)Fe]_2(\mu\text{-}CO)(\mu\text{-}\eta^1:\eta^2\text{-}CH{=}CH_2)^+$ (1) that retains an iron–iron bond.

1. Introduction

Vinyl ligands that bridge two metal centers of bimetallic and trimetallic cluster complexes almost invariably retain metal–metal bonding and/or other bridging ligands across the μ-alkenyl linkage [1,2]. For example, both an iron–iron bond and a bridging carbonyl complement the $\mu(\eta^1:\eta^2\text{-}CH{=}CH_2)$ bridging vinyl on the stereochemically non-rigid complex $[Cp(CO)Fe]_2(\mu\text{-}CO)(\mu\text{-}CH{=}CH_2)^+$ (1) [3a,b]). Equilibrating its structures **1a** and **1b** represents the established pathway for μ-alkenyl ligand oscillation, sometimes described as a windshield wiper motion [4], that exchanges the environments of the CpFe(CO) centers. This fluxional process shifts the alkenyl β-carbon between the iron centers as the α-carbon remains bonded to both irons; the β-hydrogens H_A and H_M neither interconvert with themselves nor with the α-hydrogen H_X [4]. The 1,2-diiron bicyclobutane representations **1a** and **1b** also conform with a finite μ-carbenoid bonding contribution at this C_α-site [5], as deduced from X-ray crystallography [3c] and NMR spectral [3b,d,e] arguments for **1** and for a number of other σ,π-alkenyl compounds [5].

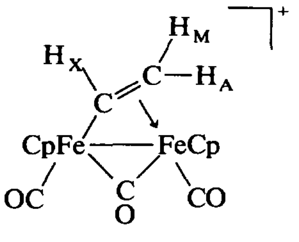

(1)

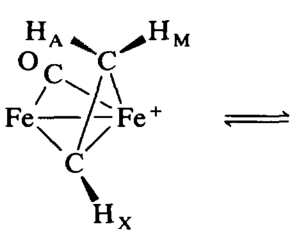

(1a)

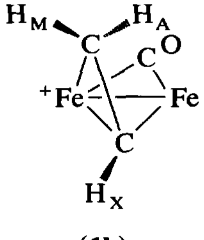

(1b)

The $\mu(\eta^1:\eta^2)$ vinyl compound $(Fp{-}CH{=}CH_2)Fp^+$-BF_4^- (3) differs from **1** by the lack of a constraining metal–metal bond or other bridging ligand. We now report the synthesis (eqn. (1)) and characterization of

---

Correspondence to: Professor A.R. Cutler.

0022-328X/93/$6.00

3, which included evaluating its fluxional properties by ^1H NMR magnetization transfer experiments. The ease of μ-vinyl ligand oscillation between the Fp centers on **3** will be compared with that established for **1**.

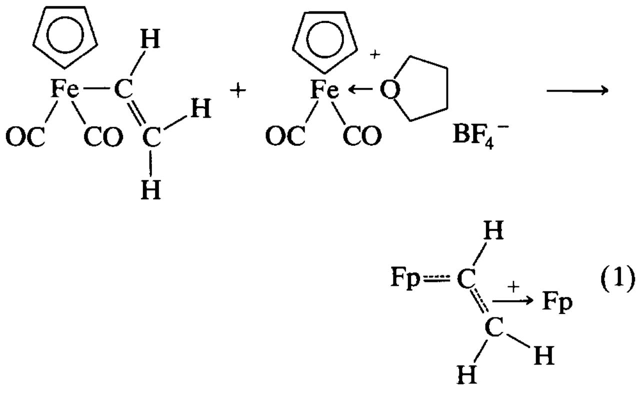

(1)

(3)

2. Experimental section

Synthetic manipulations were performed using standard Schlenk line procedures for working in an inert nitrogen atmosphere [6]. Infrared spectra of methylene chloride solutions were recorded on Perkin–Elmer spectrophotometers, Model Nos. 297 and 1600 (FT), for the carbonyl ν(CO) absorptions (2200–1600 cm^{-1}). NMR spectral data (δ values in ppm downfield from internal TMS) were obtained in acetone-d_6 or nitromethane-d_3 solutions using Varian Model XL-200 and IBM-WP100 spectrometers. Combustion microanalyses were done by Desert Analytics, Tucson, AZ.

Organic and inorganic reagents were obtained commercially and used as received. Dichloromethane was distilled under nitrogen from P_2O_5; THF was distilled from sodium benzophenone ketyl. The Fp starting materials Fp_2 [7], $Fp(THF)^+BF_4^-$ [8], and $FpCOCH=CH_2$ [9] were prepared by literature procedures and judged pure by IR and ^1H NMR spectroscopy. A modification of King's procedure [9] was used to prepare $FpCH=CH_2$ (20% yield) by photolysis of $FpCOCH=CH_2$ in dichloromethane at 5°C. Authentic samples and spectral data of $FpCH_2CHCH_2Fp^+BF_4^-$ (**4**) [10], $(FpCH_2CH_2CH=CH_2)Fp^+BF_4^-$ (**5**) [10], $Fp(CH_2=CHCH_3)^+BF_4^-$ [11], $Fp(CH_2=CHOCH_3)^+BF_4^-$ [12] and $FpCH_2CH_3$ [11a] were available from previous studies for direct comparison.

2.1. Synthesis of $[Cp(CO)_2FeCH=CH_2]Fp^+BF_4^-$ (3)

A dichloromethane solution (50 ml) containing $FpCH=CH_2$ (2.00 g, 0.010 mol) and $Fp(THF)^+BF_4^-$ (2.50 g, 0.011 mol) was refluxed gently for 14 h. After cooling to room temperature, the resulting dark red solution was added dropwise to 200 ml of pentane, and the yellow-orange precipitate was filtered. This solid was reprecipitated from acetone (20 ml)/pentane (100 ml layer), filtered, and vacuum dried to give a yellow solid (3.20 g) that was identified as $(FpCH=CH_2)Fp^+$-BF_4^- (**3**) (71% yield). IR (CH_3NO_2): 2060, 2030, 2018, 1982 cm^{-1} (CO). ^1H NMR (CD_3NO_2) δ 7.53 (dd, $J = 8.1$, 16.5 Hz, Fe-C*H*=CH_2); 5.52 (s, η^2-Fp^+); 5.38 (s, η^1-Fp); 4.67 (d, $J = 8.1$ Hz, *E*-Fp-CH=C*H*H); 3.37 (d, $J = 16.5$ Hz, *Z*-Fp-CH=CH*H*); ^{13}C NMR (acetone-d_6) (gated decoupled) δ 215.65, 214.18, 213.85, 212.78 (CO); 133.18 (d, $^1J(CH) = 148.9$ Hz, Fp*C*H=CH_2); 89.53, 89.33 (Cp, ^1H decoupled); 63.29 (t, $^1J(CH) = 153.6$ Hz, Fp-CH=*C*H_2). Anal. Found: C, 41.21; H, 2.92. $C_{16}H_{13}O_4FeBF_4$ calc.: C, 41.08; H, 2.80%.

2.2. Reaction of $[Cp(CO)_2FeCH=CH_2]Fp^+BF_4^-$ (3) and PPh_3

A suspension of $(FpCH=CH_2)Fp^+BF_4^-$ (**3**) (206 mg, 0.50 mmol) in 20 ml of dichloromethane was treated with PPh_3 (183 mg, 0.70 mmol) at room temperature. IR spectral monitoring of the yellow-brown solution that formed within 0.5 h was consistent with quantitative transformation of **3** to a Fp species with ν(CO) bands at 2061, 2018, 1962 cm^{-1}. Dropwise addition of this solution into 125 ml of ether afforded a pale yellow precipitate, which was filtered, washed with ether, vacuum dried, and identified as Fp-$PPh_3^+BF_4^-$ [13] (300 mg, 87% yield). ^1H NMR (CD_3NO_2): δ 5.38 (d, $J = 0.5$ Hz, Cp); 7.57 (br s, PPh_3). IR (CH_2Cl_2): 2061, 2018 cm^{-1} (CO).

The filtrate was evaporated and extracted with pentane (5 × 3 ml). These combined extracts were filtered through activity III alumina (5 × 2 cm diameter column) with pentane. The resulting yellow eluate was evaporated to a yellow-brown oil that was identified as $FpCH=CH_2$ [9] (190 mg, 81% yield). IR (CH_2Cl_2): 2018, 1960 cm^{-1} (CO). ^1H NMR (C_6D_6): δ 7.17 (dd, $J = 17.1$, 9.0 Hz, Fp-C*H*=CH_2); 4.04 (Cp); 6.26 (dd, $J = 8.9$, 0.9 Hz, *E*-Fp-CH=C*H*H); 5.76 (dd, $J = 17.1$, 0.9 Hz, *Z*-Fp-CH=CH*H*).

2.3. Measurement of spin-lattice relaxation times of $(Fp$-$CH=CH_2)Fp^+BF_4^-$ (3)

A solution of $(FpCH=CH_2)Fp^+BF_4^-$ (**3**) (25 mg) in acetone-d_6 (0.4 ml), which previously had been degassed by three freeze-pump-thaw cycles on a vacuum line, was transferred in a glove box to a 5 mm NMR tube and sealed with a rubber septum. A standard inversion recovery pulse sequence using an acquisition time of 3.09 s and a D1 delay time of 40.00 s was applied to the sample at 25.2°C. The Varian exponential data analysis program provided the semilogarith-

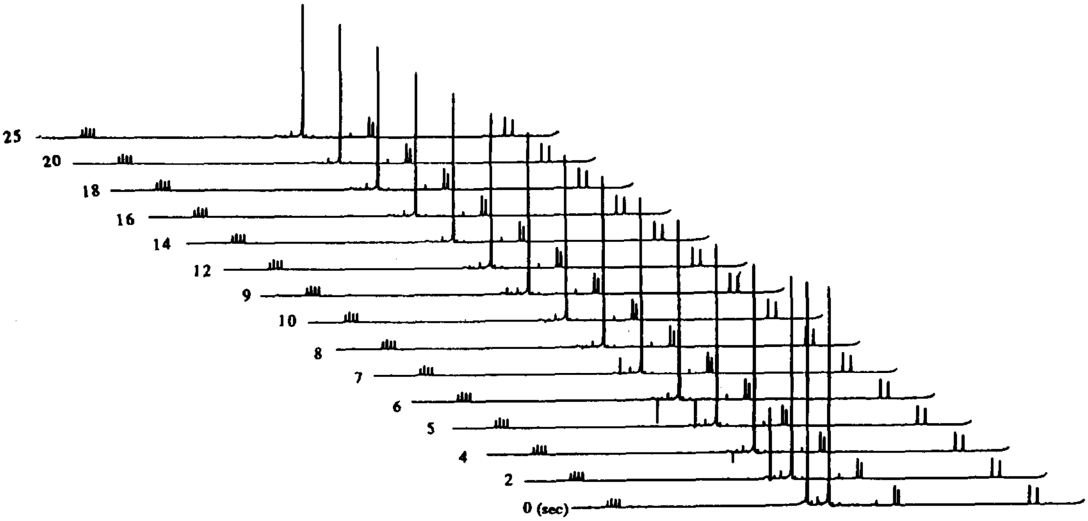

Fig. 1. Spin saturation transfer ^{1}H NMR spectra of $(Fp{-}CH{=}CH_2)Fp^+BF_4^-$ (3) in acetone-d_6 (25°C). Stacked spectral plots represent fourteen intervals during which the downfield Cp resonance was saturated. The bottom scan is a normal spectrum ($t = 0$).

mic fit of the peak intensity $(I_\infty - I_t)$ *vs.* time data that provided the T_1 values: δ 7.72 (dd, $T_1 = 4.03 \pm 0.12$ s); 5.72 (Cp, $T_{1B} = 9.09 \pm 0.15$ s); 5.49 (Cp, $T_{1A} = 10.33 \pm 0.30$ s); 4.79 (d, $T_1 = 1.69 \pm 0.09$ s); 3.36 (d, $T_1 = 2.22 \pm 0.05$ s).

2.4. Magnetization transfer experiments: method of spin saturation transfer

An acetone-d_6 solution (0.4 ml) of $(FpCH{=}CH_2)Fp^+BF_4^-$ (3) (25 mg), prepared as noted above, was examined using as a presaturation pulse sequence: D2, PW, acquisition, D1. D1 was set as a 40 s preparation time, and D2 controlled the gating of a selective decoupling pulse that progressed in 15 intervals from 0 to 38 s. The downfield Cp singlet (δ 5.72) corresponding to the $Fp(\eta^2\text{-vinyl})^+$ group was selectively decoupled. At the end of D2, the decoupler was turned off and the normal sequence of proton observation was initiated. (PW was set as a 90° observation pulse and the acquisition time was set at 3.09 s for a sweep width of 2600 Hz.) Figure 1 depicts the resulting 15 stacked NMR spectra.

The NMR signal intensities were analyzed using eqn. (2) [14].

$$M_A(t) = M_A^\infty + M_A^\circ[\tau_{1A}/\tau_A]\exp[-t/\tau_{1A}] \qquad (2)$$

$M_A(t)$ is the magnetization at time t for the protons A undergoing magnetization transfer from a second set of nuclei, B, which are linked by chemical exchange to A and are subjected to a saturating RF field. M_A^∞ represents the steady-state magnetization for the protons A due to saturation of B; M_A° is the equilibrium magnetization in the absence of saturation of B. The average lifetime of the spin state for a nucleus at site A, τ_{1A}, is related to the spin-lattice relaxation time of A, T_{1A}, and to the inverse of the first-order exchange rate

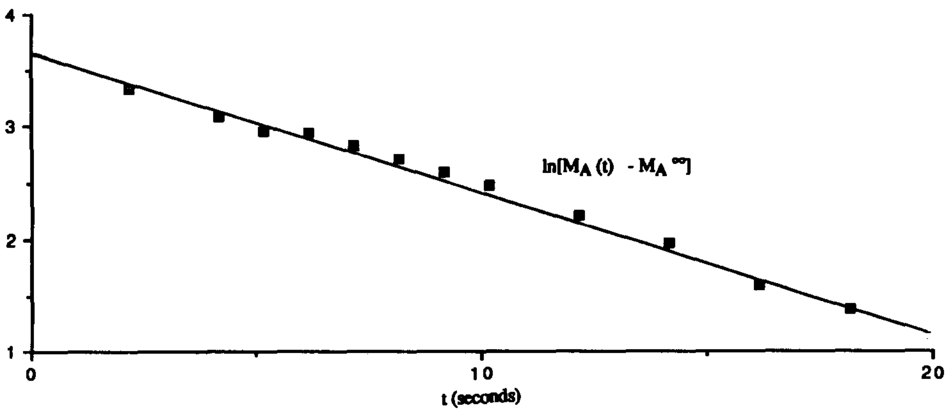

Fig. 2. Plot of $\ln[M_A(t) - M_A^\infty]$ *vs* t (the interval of saturation) for the data in Fig. 1.

constant, τ_A (which interconverts sites A and B) by the expression, $1/\tau_{1A} = 1/T_{1A} + 1/\tau_A$.

Operationally, A corresponds to the Cp hydrogens that resonate at 5.49 ppm, whereas B denotes the Cp resonance at 5.72 ppm. M_A^∞ was obtained as the minimum signal intensity of A after saturating B for 40 s. (The slope of a typical $M_A(t)$ *vs*. t plot was invariant after 25 s.) M_A° was determined from the results of a control experiment in which the same decoupler (saturating) pulse was moved 45 Hz upfield of A and the resulting equilibrium magnetization of A (which remained constant over 10–40 s) was measured. A least-squares fit to the plot of $\ln[M_A(t) - M_A^\infty]$ *vs* t (Fig. 2) established a value for $\tau_{1A} = 8.17$ s from the slope ($-1/\tau_{1A} = -0.0117$; least-squares correlation coefficient $r = -0.990$). A corresponding value for $T_{1A} = 12.41$ s from the relationship $T_{1A} = \tau_{1A} M_A^\circ / M_A^\infty$ was used in eq. (3) in order to calculate the first-order exchange rate constant 0.045 s^{-1}.

$$k_{AB} = (1/T_{1A})[(M_A^\circ/M_A^\infty) - 1] \qquad (3)$$

2.5. Magnetization transfer: method of inversion transfer

Standard software commands were used to selectively invert the upfield δ 5.49 Cp resonance of **3**, corresponding to the Fp(η^1-vinyl) group (in acetone-d_6, 25°C) and then to incrementally delay the 90° observation pulse (1.54 s acquisition time/2600 Hz spectral width) by programmed intervals $t = 0.01$–20 s. Decoupler power and pulse-width settings for the selective 180° pulse were optimized in order to maximize peak inversion at δ 5.49 ppm. The 32 transients that were sampled for each interval were divided into four blocks of eight transients, and the blocks were acquired in a rotating sequence during the 12 h experiment. Spectral data was analyzed and plotted in the difference mode by subtracting the spectral scan corresponding to each interval t from the fully relaxed spectrum, which was obtained during the same experiment.

The peak intensity data was analyzed by the procedure of Dahlquist *et al.* [15]. Equations (4) and (5) were used to plot the data; $M_A(t)^*$ and $M_B(t)^*$ denote peak heights for the inverted Cp resonance A (δ 5.49) and the exchanging Cp signal B (δ 5.72) as they appear in the difference spectra. The sum $[M_A(t)^* + M_B(t)^*]$ indentifies the total magnetization introduced by the selective pulse, which relaxes at a rate T_{1A}^{-1}, and the difference $[M_A(t)^* - M_B(t)^*]$ measures the equilibration of excess magnetization between Cp sites due to T_1 relaxation. Figure 3 collects graphs of the plots

$$[M_A(t)^* + M_B(t)^*] = M_A^\circ[-t/T_{1A}] \qquad (4)$$

$$[M_A(t)^* - M_B(t)^*] = M_A^\circ \exp[(-1/T_{1A}) + k_{AB} + k_{BA}]t \qquad (5)$$

of $\ln[M_A(t)^* + M_B(t)^*]$ and $\ln[M_A(t)^* - M_B(t)^*]$ *vs*. intervals t. The slope of the former plot is -0.141 ($r = 1.000$), which provided a value for $T_{1A} = 7.1$ s. The slope of the latter plot is -0.240 ($r = 0.999$), which gave $k_{AB} = k_{BA} = 0.049$ s^{-1}.

3. Results and discussion

3.1. Characterization of $Cp(CO)_2Fe$-(μ-η^1:η^2-$CH{=}CH_2$)$Fe(CO)_2Cp^+BF_4^-$ (3)

Treatment of the known [9] η^1-vinyl complex Fp–$CH{=}CH_2$ with the labile Lewis acid precursor $Fp(THF)^+BF_4^-$ [8] afforded the μ-vinyl compound $(Fp{-}CH{=}CH_2)Fp^+BF_4^-$ (**3**) (eqn. (1)) in moderate yield. Reprecipitation from acetone/pentane or acetone/ether deposited analytically pure **3**, a stable material that varies in appearance from a dark yellow-brown microcrystalline solid to a brown powder. Subse-

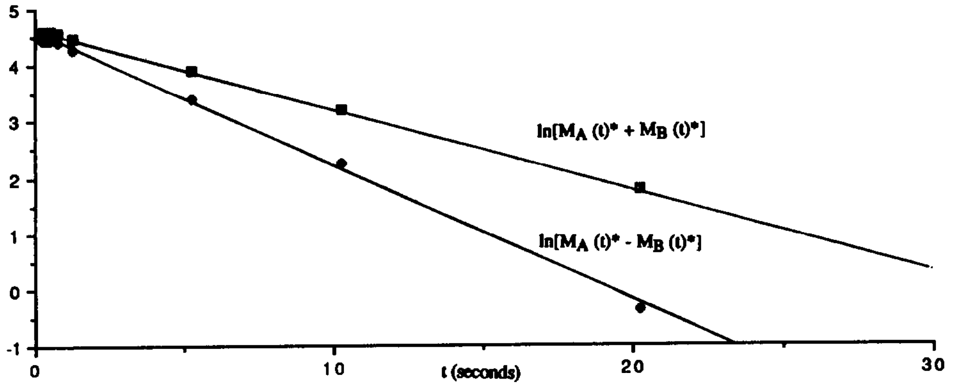

Fig. 3. Inversion (magnetization) transfer plots of $\ln[M_A(t)^* + M_B(t)^*]$ and $\ln[M_A(t)^* - M_B(t)^*]$ *vs* interval t (in seconds). Values along the ordinate are in arbitrary peak intensity units.

quent attempts at crystallizing **3** as its BF_4^-, PF_6^-, and BPh_4^- salts invariably gave brownish powders.

The ligand exchange that is implicit in the synthesis of **3**, a standard method for coordinating alkenes as $Fp(\eta^2\text{-alkene})^+$ compounds [11b], previously had been used in preparing several bimetallic compounds that are relevant to the present study. Thus, the bis-Fp μ-(1,3-propenyl) **4** [16d,e] and the bis-Fp μ-($\eta^1:\eta^2$) butenyl **5** [10,16g,17] were obtained by treating the appropriate σ-complex with $Fp(THF)^+$ or another Fp^+ Lewis acid precursor. Giering also briefly communicated the synthesis of the bis-Fp μ-($\eta^1:\eta^2$)butadienyl **6** [18], the vinylogous homolog of **3**, from protonating the bis-Fp (1,3-butadienyl) complex Fp–CH=CHCH=CH–Fp [18].

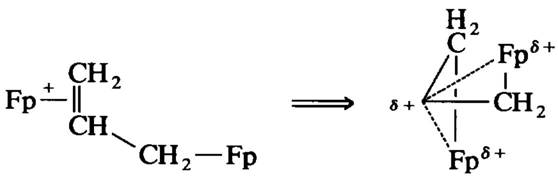
(4) **(4a)**

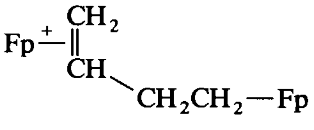
(5)

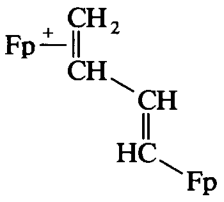
(6)

TABLE 1. IR and ^{13}C NMR spectral data

Compound	IR [a] ν(CO) (cm^{-1})		^{13}C NMR [b] $\delta(C_\alpha)$	$[^1J(C_\alpha H)]$	$\delta(C_\beta)$	$[^1J(C_\beta H)]$
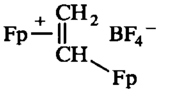	2059 2018	2029 1972	63.2	[153.6]	133.2	[148.9]
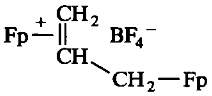	2056 1969 [c]	2020	26.8		192.0 [d]	
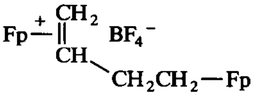	2072 2007	2034 1949	52.6	[161.7]	87.4	
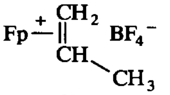	2074	2036	55.8	[167]	85.7	[159] [e]
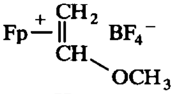	2066	2026	26.5	[160.1, 165.2]	145.0	[190.9]
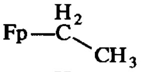	2001	1942	−2.8		21.3	
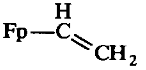	2018	1960	130.5 [f]		140.7	
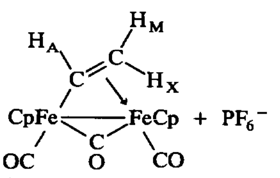	2037 [g] 1863	2012	64.2		185.8	

[a] Data recorded in CH_2Cl_2. [b] Acetone-d_6. [c] CH_3NO_2; relative m-s-m intensities consistent with the 2020 cm^{-1} absorption as a supposition of two ν(CO) bands. [d] CH_3NO_2, rapid exchange on NMR time scale affords equivalent C_α sites and a single Cp resonance [16]. [e] ^{13}C NMR data (CD_3NO_2) taken from ref. 11b. [f] ^{13}C NMR assignments (CD_2Cl_2) not verified. [g] IR and NMR data for *cis*-**1a**/**1b** [3].

Spectroscopic data for μ-($\eta^1:\eta^2$)-**3** is in accord with an unsymmetric π-complex, analogous to that established for Fp(η^2-$CH_2{=}CHOCH_3$)$^+$ (**7**) [19], that also significantly delocalizes its charge over the two structurally distinct iron centers. Tables 1 and 2 collect spectral data for **3**, as well as that of its homologs [Fp–$(CH_2)_n$CH=CH_2]Fp$^+$ (**4**) (n = 1) [10,16], (**5**) (n = 2) [10,16g,17], and other model compounds. Structurally distinct Fp centers on **3** are immediately apparent from the presence of separate ^{1}H NMR Cp resonances and of separate sets of IR ν(CO) bands for the two Fp groups. Since the carbonyls on each Fp center are diastereotopic (due to the presence of the prochiral, η^2-monosubstituted alkene) [11b], the ^{13}C NMR spectrum of **3** shows four carbonyl absorptions.

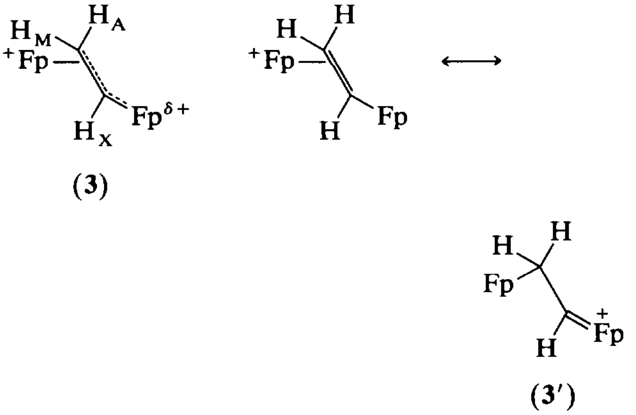

(3)

(3′)

Charge delocalization involving the two iron centers on **3** follows from comparing the IR ν(CO) spectral data [19a,c,20] with that of its homologs **4** and **5** [16g,21]. The bis-Fp μ-($\eta^1:\eta^2$) butenyl complex **5** has electronically isolated cationic Fp(η^2-alkene)$^+$ and neutral Fp(η^1-vinyl) centers on **5**: its IR spectral data matches that of the separate Fp(η^2-propene)$^+$ and $FpCH_2CH_3$ (or $FpCH{=}CH_2$) complexes, respectively. In contrast, the iron centers on the bis-Fp propenyl cation **4** delocalize the charge: their ν(CO) band energies almost converge since the Fp groups are nearly equivalent (*cf.* **4a**) on the IR timescale. For **3**, the two higher energy Fp(η^2-alkene)$^+$ ν(CO) bands and the two remaining Fp(η^1-alkyl) ν(CO) bands resemble those for **4**. Moreover, both **3** and **4** exhibit the same 87 cm^{-1} spread in ν(CO) frequencies, in contrast to the maximum $\Delta\nu$(CO) of 123 cm^{-1} for **5**. It is also worth noting that the Fp(η^2-alkene)$^+$ ν(CO) band energies of **3** are close to

TABLE 2. ^{1}H NMR spectral data [a]

Compound	δ(Cp)	$\delta(H_A)$	$\delta(H_M)$	$\delta(H_X)$	$^3J_{AX}$	$^3J_{MX}$	$^3J_{AM}$
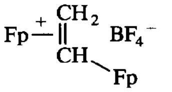 $Fp\overset{+}{-}\|\!\|(CH_2{=}CH{-}Fp)\ BF_4^-$	5.72 [b] 5.49	3.36	4.79	7.72	16.4	8.1	[c]
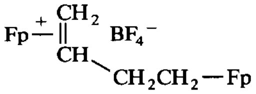 $Fp\overset{+}{-}\|\!\|(CH_2{=}CH{-}CH_2CH_2{-}Fp)\ BF_4^-$	5.85 [b] 4.98	3.49	3.93	5.38	14.7	8.1	[c]
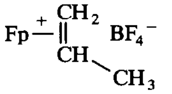 $Fp\overset{+}{-}\|\!\|(CH_2{=}CH{-}CH_3)\ BF_4^-$	5.85	3.63	4.04	5.33	14.7	8.4	[c]
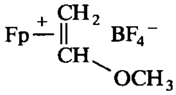 $Fp\overset{+}{-}\|\!\|(CH_2{=}CH{-}OCH_3)\ BF_4^-$	5.68	2.88	3.14	8.01	4.5	11.9	2.4
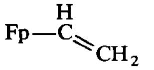 $Fp{-}C(H){=}CH_2$	4.71 [d]	5.24	5.71	6.80	17.1	8.9	0.95
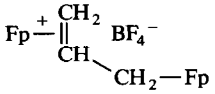 $Fp\overset{+}{-}\|\!\|(CH_2{=}CH{-}CH_2{-}Fp)\ BF_4^-$	5.50 [e]						
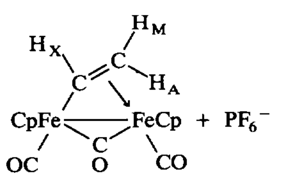 + PF_6^-	5.79 [b] 5.58	3.01	5.19	12.70	13.2	7.4	[c]

[a] Data recorded in acetone-d_6. [b] Downfield Cp singlet assigned to CpFe(η^2-vinyl)$^+$ group. [c] Not observed. [d] $CDCl_3$. [e] Data taken from ref. 16b; fluxional: C_3H_5 is AX_4 at 20°C and A_2B_2X between −10°C and −70°C.

those of the charge delocalized Fp(η^2-vinyl ether)$^+$ salt **7**.

^{1}H NMR spectral data for **3** are also consistent with charge delocalization between the two Fp centers [20]. Chemical shifts for the Cp ligands on **3**, δ 5.72 for the Fp(η^2-alkene)$^+$ and δ 5.49 for the Fp(η^1-vinyl) groups, lie between those for the Cp ligands on ($FpCH_2CH_2CH{=}CH_2$)$Fp^+BF_4^-$ (**5**) (Table 2) or on Fp(η^2-propene)$^+$ and $FpCH_2CH_3$ complexes (δ 5.85 and 4.87, respectively, all in acetone-d_6). Also, the Fp(η^2-alkene)$^+$ δ Cp value of **3** is close to that of the charge delocalized Fp(η^2-vinyl ether)$^+$ salt **7**.

The carbenoid resonance form **3′** evidently does not significantly contribute to **3**, as deduced from ^{1}H and ^{13}C NMR spectral data. ^{1}H NMR spectral data for **3** identifies a vinyl AMX spin system that resembles those of other Fp(monosubstituted alkene)$^+$ [11] and vinyl [22] complexes. Both the presence of this spin system on **3** and especially its H_X chemical shift are inconsistent with the carbenoid resonance form **3′**, which should afford a downfield shift greater than δ 10 [23] for H_X. The ^{13}C NMR chemical shift for the vinyl C_β site on **3**, δ 133, falls in between values (Table 1) for similar Fp(alkene)$^+$ sites on **5** or Fp(propene)$^+$ and on Fp($CH_2{=}CHOCH_3$)$^+$ (**7**). This ^{13}C NMR chemical shift should approach 300 ppm if a carbenoid site [24] analogous to that on **3′** significantly contributes to **3**.

Structures analogous to **3′** are known in which replacing an α-H by a heteroatom favors the carbenoid resonance form. For example, Akita *et al.* [25] have used NMR spectral data in describing the structure of $FpCH_2C(OCH_3)Fp^+$. Its ^{13}C NMR chemical shift for the C_β (carbenoid) site at 299 ppm is consistent with **8** as the predominate resonance contributor. Other $FpCH_2C(X)Y^+$ complexes containing a single Fp center delocalize the C_β charge through one or more heteroatoms and a through-space interaction with the iron center (the β-effect) [26]. These complexes typically exhibit lower chemical shifts for C_β: $FpCH_2C(OCH_3)_2^+$ (δ 200) and $FpCH_2CH[N(CH_3)_2]^+$ (δ 178) [19c].

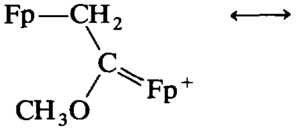

(**8**)

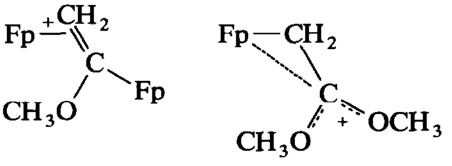

The chemical reactivity of **3** resembles that of a Fp(alkene)$^+$ complex. Thus, treatment of **3** with triphenylphosphine cleanly afforded Fp(vinyl) and $FpPPh_3^+$ [13] (eqn. (6)) as the only detectable organoiron products by IR and ^{1}H NMR spectroscopy.

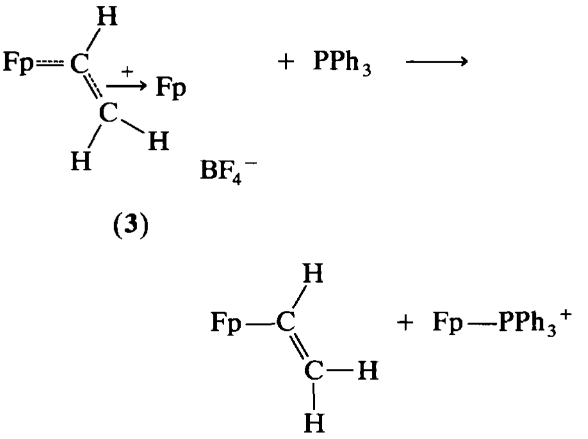

(6)

The isolated yields were 81% and 87% respectively. Similar nucleophilic displacement of alkene from Fp(η^2-alkene)$^+$ complexes is well established; PPh_3, for example, readily displaces propene from Fp($CH_2{=}CHCH_3$)$^+$ [11a,27]. Fp(alkylidene)$^+$ complexes, in contrast, would add PPh_3 to the carbenoid carbon, as has been demonstrated for $Cp[P(OPh)_3](CO)Fe{=}CHCH_3^+$ transforming to $Cp[P(OPh)_3](CO)Fe{-}CH(PPh_3)CH_3^+$ [28].

The $\mu(\eta^1:\eta^2$-$CH{=}CH_2)$ or σ,π-structure that we assign to the μ-vinyl compound ($Fp{-}CH{=}CH_2$)Fp^+ BF_4^- (**3**) differs from that previously established for the bis-Fp μ-(1,3-propenyl) salt **4** [16]. IR spectral evidence and the results of an X-ray crystallographic structure determination of **4** are consonant with the presence of nonequivalent η^1-bonded Fp groups, both evidently interacting with the C_β carbocation center (Fe–C_β distances are 2.59 and 2.72 Å) [16c]. Tautomer **4a** bearing two antiperiplanar Fp groups is a plausible structure [16b]. Results of variable temperature NMR spectral studies are in accord with both hindered rotation about the Fe–C_α bonds [16b] (higher energy process) and a fluxional motion that renders the iron groups equivalent on the NMR time scale. A synchronous bending displacement of the Fp groups that both maintains their *trans* antiperiplanar array [16b] and alternates the short-long Fp–C_β bonding interactions accounts for the low temperature fluxionality of **4**.

The bis-Fp $\mu(\eta^1:\eta^2)$ vinyl **3** and μ-(1,3-propenyl) **4** compounds represent a class of organobimetallic molecules that polarize charge across an intervening organic ligand system [29]. A number of these systems that also have considerable charge delocalization between CpFe groups include Casey's $\mu(\eta^1:\eta^4)$-butadiene complex **9** [30], a series of $\mu(\eta^1$-C$:\eta^1$-O)-acyl compounds **10** [29b], and several $\mu(\eta^1\text{-C}:\eta^1\text{-O})$-enolate ($R = H$, Ph, OCH_3) or $\mu_3(\eta^1\text{-C}:\eta^1\text{-O})$-ketene ($R = Fp$) complexes **11** [25]. Effective charge polarization through these conjugated ligand systems derives in part from the neutral Fp group serving as a powerful net electon donor [29a].

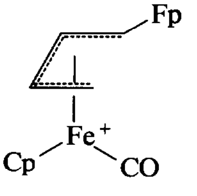

(9)

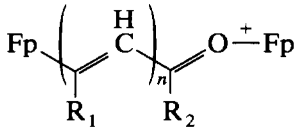

(10)

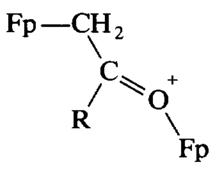

(11)

3.2. *Magnetization transfer studies*

The anticipated μ-vinyl ligand oscillation for **3** (eq. (7)) must be very slow on the NMR time scale, since separate, narrow Cp resonances are observed in its ^{1}H and ^{13}C NMR spectra. Attempts to increase this exchange rate and detect the equilibrium through peak broadening/coalescence of the Cp resonances proved unsuccessful. ^{1}H NMR spectra of **3** in CD_3NO_2 up to 65°C, just prior to it decomposing, showed no broadening. Fortunately, the dynamics of slowly exchanging organometallic systems [31] (such as **3**) are accessible by using NMR magnetization transfer procedures [14,15]. These magnetization transfer procedures are particularly useful for equilibrating systems with exchange rates that are the same order of magnitude as $1/T_1$ (T_1 = spin lattice relaxation time) [32] and are slow enough to retain resolved spectral lines for the exchanging species.

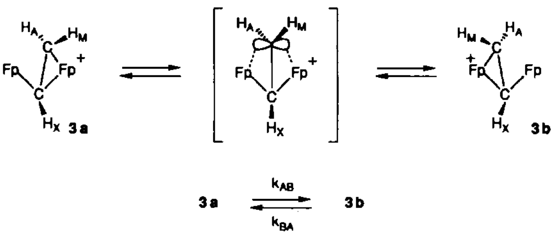

(7)

We used two ^{1}H NMR magnetization procedures, spin saturation transfer and inversion transfer, for quantifying the rate of vinyl ligand oscillation on **3**. Since this chemical exchange **3a** ⇔ **3b** (eqn. (7)) interconverts the CpFe environments, the separate Cp resonances of **3** thus define an equally populated, two-spin exchange system. In the spin saturation transfer experiment, one Cp absorption is saturated during a programmed time, and the decrease in peak intensity for the other Cp singlet (attributed in part to magnetization transfer) is measured. Analysis of this peak perturbation provides both the T_1 relaxation time and the exchange rate constant $k_{AB} = k_{BA}$. The inversion transfer procedure differs in that one Cp absorption is selectively inverted with a 180° pulse, and after a preset interval, a nonselective 90° observation pulse is applied. Relating peak intensities for both the inverted Cp absorption and the other Cp resonance that is receiving the magnetization as a function of delay interval also provides values for T_1 and for the exchange rate constant.

Implementing the spin saturation transfer experiment on **3** entailed saturating the δ 5.72 (downfield) Cp singlet, corresponding to the $Fp(\eta^2\text{-vinyl})^+$ group, for 0—25 s and then measuring the decay of the δ 5.49 Cp resonance. Stacked plots of the spectral scans over 15 time intervals (Fig. 1) illustrate the 39% decrease in intensity of the upfield Cp resonance, in contrast to < 4% fluctuation in intensity of the vinyl absorptions. The bottom spectral scan is the unperturbed ^{1}H NMR spectrum of **3** in acetone-d_6. Analysis of the data as outlined in the Experimental section afforded the first order rate constant for exchange, $k_{AB} = 0.045\ s^{-1}$.

The magnitude of k_{AB} depends on the value of T_{1A}, the spin lattice relaxation time of the Cp resonance (δ 5.49) receiving the magnetization transfer, that is used in eqn. (3). The value used, $T_{1A} = 12.4$ s, came from analysis of the magnetization transfer data. A standard inversion recovery pulse sequence was used to measure independent T_1 values for the Cp resonances at δ 5.72 (9.1 s) and δ 5.49 (10.3 s) for **3**.

Two control experiments were carried out in order to validate the results of the saturation transfer experiment. The first entailed moving the decoupling pulse 45 Hz upfield of the δ 5.49 Cp signal and irradiating at the same (saturating) power level. Irradiating at this new position (in a region devoid of extraneous NMR signals) maintains the frequency difference between the δ 5.72 and δ 5.49 Cp signals. Since the intensity of the δ 5.49 Cp signal remained unchanged during this control, the possibility of stray radiation reducing the intensity of the δ 5.49 Cp singlet while saturating the δ 5.72 Cp absorption can be eliminated.

A second set of control experiments were needed to determine if nuclear Overhauser effects also contributed to the intensity of the Cp signal for the Fp group receiving magnetization transfer. Distinguishing between these two contributions to the signal intensity requires lowering the sample temperature until chemical exchange stops; NOE enhancements should not be effected. We did variable temperature (−30°C to +25°C) NOE difference spectroscopy experiments [33] on **3** (toluene-d_8) in which the two Cp and the three vinyl absorptions were sequentially and selectively saturated. The results of these experiments demonstrated: (1) that chemical exchange **3a** ⇔ **3b** was not detected below −5°C, (2) that NOE enhancements between the Cp groups were absent below −5°C (and presumably also at higher temperature), and (3) that the vinyl hydrogens exhibited mutual NOE interactions, but did not exchange with one another at room temperature. Perhaps the best confirmatory evidence for the spin saturation transfer results corresponds to the outcome of the inversion transfer pulse sequence.

The inversion (magnetization) transfer experiment was carried out by perturbing the other (upfield) Cp resonance of **3** at δ 5.49 Cp. The resulting spectral data were processed as difference spectra for the programmed delay times and were analyzed by the procedure of Dahlquist *et al.* [15] (eqns. (4) and (5)). This process afforded values of the exchange rate constant $k_{AB} = k_B = 0.049\ s^{-1}$ and for the relaxation time $T_{1A} =$ 7.1 s.

The reasonable agreement between the k_{AB} measurements (0.045 and 0.049 s^{-1}) that we obtain from two different magnetization transfer experiments does not carry over to their corresponding T_{1A} results. T_{1A} values of 12.4 and 7.1 s originating from the spin saturation transfer and inversion transfer experiments, respectively, also do not match our independently measured (via inversion recovery) $T_{1A} = 10.3$ s and $T_{1B} = 9.9$ s. This discrepancy in measured T_1 values must represent a source of error; furthermore, $T_{1A} = T_{1B}$ is required by the analytical procedures [14,15,34] that we used for both types of magnetization transfer experiments. Since we probably have not reduced all systematic errors sufficiently for random errors to dominate, statistical limits of errors on the values of k_{AB} accordingly have not been given.

3.3. *μ-Vinyl ligand oscillation on* $(FpCH{=}CH_2)Fp^+$ *(3) and on* $[Cp(CO)Fe]_2(\mu\text{-}CO)(\mu\text{-}CH{=}CH_2)^+$ *(1)*

Comparing the μ-vinyl ligand oscillation for **1** and **3** would help assess the role of the iron–iron bond in **1** in facilitating this fluxional motion. Presence of the iron–iron bond could enhance the μ-vinyl ligand oscillation, since the bimetallobicyclobutonium structure for **1** resembles the isolobal organic bicyclobutonium carbonium ions. These bicyclobutonium ions also enter a manifold of rapid degenerate rearrangements [35] that resemble in part the μ-vinyl ligand windshield wiper motion. In addition, the iron–iron bond in **1** engenders a lower energy *cis* → *trans* isomerization (with respect to the structural disposition of the Cp ligands) that does not apply to **3**.

Only fragmentary NMR spectral data are available for **1**, which limits comparing the fluxionality of **1** and **3**. Attempts to quantify the μ-vinyl ligand oscillation of **1** by a dynamic ^1H NMR peak broadening/coalescence temperature procedure only established that the separate Cp resonances (of the lower energy *cis* isomer) only began broadening at the 50° decomposition temperature [3b].

A lower limit to the activation energy for the two-site exchange of the μ-vinyl ligand on **1** can be calculated by using the Eyring equation, $k_{AB} = (\kappa kT/h) \exp(-\Delta G^\ddagger/RT)$, where k is the Boltzmann constant, h is Planck's constant, and $\kappa = 1$ represents the transmission coefficient [14b]. Approximate values for k_{AB} are conveniently obtained from NMR spectral data and the relationship $k_{AB} = 2.22(\Delta\nu)$ (ideally at the coalescence temperature T_c), where $\Delta\nu$ is the stopped-exchange separation of the Cp resonances. Casey used this procedure and ^1H NMR spectral data for **1** ($\Delta\nu =$ 57 Hz) at 27°C [3f] to approximate a minimum value of $\Delta G^\ddagger \geq 14.7$ kcal/mol, which fortuitously is the same minimum value that we calculate for **3** ($\Delta\nu = 45$ Hz) at 25°C. Substituting the higher temperatures that **1** and **3** were heated (50°C and 65°C), but which apparently are still $< T_c$, generate somewhat higher values of $\Delta G^\ddagger \geq$ 16.6 and 16.8 kcal/mol, respectively. A more accurate determination of $\Delta G^\ddagger = 19.3$ kcal/mol for vinyl oscillation on **3** results from substituting $k_{AB} = 0.045\ s^{-1}$ into the Eyring equation (25°C).

We believe that a minimum value of $\Delta G^\ddagger \geq 16\text{–}17$ kcal/mol for the vinyl fluxionality of **1** is a reasonable approximation. Knox observed that 50°C apparently is close to the T_c for **1**, although another 10°C increase for T_c only increases $\Delta G^\ddagger$ to 17.2 kcal. It is worth noting that the presence of alkyl and acyl substituents on the alkenyl ligand as homologs of **1** enhance the rate of this σ,π-interchange; typical values of $\Delta G^\ddagger$ range between 10 and 13 kcal/mol. Our value of $\Delta G^\ddagger = 19.3$ kcal/mol for **3** therefore indicates that a constraining metal–metal bond on **1** does not appreciably facilitate μ-vinyl oscillation, and absence of this bond on **3** only raises this fluxional barrier by approximately 2–3 kcal/mol.

4. Conclusions

The $\mu(\eta^1:\eta^2)$ vinyl complex $(Fp\text{–}CH{=}CH_2)Fp^+$ PF_6^- (**3**), lacking a Fe–Fe bond, retains an unsymmetric π-complex structure in which positive charge is delocalized over the spectroscopically distinct iron centers. A comparison of its IR and NMR spectral data with that of appropriate reference compounds (Tables

1 and 2) indicates that a carbenoid resonance form $Fp-CH_2CH{=}Fp^+$ (**3'**) does not significantly contribute to the bonding. In spite of the high charge polarization between the Fp centers on **3**, its reaction with PPh_3 (displacement of $FpCH{=}CH_2$, eqn. (6)) resembles that of other $Fp(\eta^2\text{-alkene})^+$ compounds. A further assessment of this charge polarization will be possible once samples of $[Fp-CH{=}CH-(CH{=}CH)_n-CH{=}CH_2]Fp^+$, homologs of **3**, become available.

The μ-vinyl complex **3** is fluxional at room temperature, although the μ-vinyl oscillates between the Fp centers (eqn. (7)) slowly on the NMR time scale. Two ^1H NMR magnetization transfer studies using spin saturation transfer and inversion transfer procedures for the separate Cp resonances arrived at a first-order exchange rate constant $k_{AB} = 0.045\text{–}0.049\ s^{-1}$. This fluxional motion swaps the Fp centers, whereas the vinyl hydrogens engage in only mutual NOE interactions and not site exchange under similar conditions. The calculated free energy of activation for this fluxionality, $\Delta G^{\ddagger} = 19.3$ kcal/mol, appears to be 2–3 kcal/mol higher than is estimated as a minimum value for the corresponding μ-vinyl complex $[Cp(CO)Fe]_2(\mu\text{-}CO)(\mu\text{-}\eta^1:\eta^2\text{-}CH{=}CH_2)^+$ (**1**), which retains an iron–iron bond. Nevertheless, the presence of a constraining metal–metal bond (or indeed of other bridging ligands) is not a prerequisite for μ-vinyl ligand oscillation.

Acknowledgements

Support from the Department of Energy, Office of Basic Energy Sciences is gratefully acknowledged. We also thank Thomas Forschner and Alicia Todaro for contributing preliminary observations and for their interest in this work.

References

1 (a) J. Holton, M. F. Lappert, R. Pearce and P. I. W. Yarrow, *Chem. Rev., 83* (1983) 135; (b) Selected references: H. Suzuki, H. Omori and Y. Moro-oka, *Organometallics,* 7 (1988) 2579; M. J. Chetcuti, J. C. Gordon, K. A. Green, P. E. Fanwick and D. Morgenstern, *Organometallics, 8* (1989) 1790; Y. Ramon, J. Ros, I. Moldes, R. Mathieu, S. Xavier and M. Font-Bardia, *J. Chem. Soc., Dalton Trans.*, (1990) 3147 and refs. therein.

2 Relevant exception, $(CO)_5Re\text{-}[\mu\text{-}(\eta^1:\eta^2)\text{-}CH{=}CH_2]\text{-}Re(CO)_5{}^+BF_4{}^-$: P. Steil, W. Beck and F. G. A. Stone, *J. Organomet. Chem., 368* (1989) 77 and refs. therein.

3 (a) S. C. Kao, P. P. Y. Lu and R. Pettit, *Organometallics, 1* (1982) 911; (b) A. F. Dyke, S. A. R. Knox, M. J. Morris and P. J. Naish, *J. Chem. Soc., Dalton Trans.*, (1983) 1417, (c) A. G. Orpen, *J. Chem. Soc., Dalton Trans.*, (1983) 1427; (d) C. P. Casey, S. R. Marder and B. R. Adams, *J. Am. Chem. Soc., 107* (1985) 7700; (e) B. P. Gracey, S. A. R. Knox, K. A. Macpherson, A. G. Orpen and S. R. Stobart, *J. Chem. Soc., Dalton Trans.*, (1985) 1935; (f) C. P. Casey, E. A. Austin and A. L. Rheingold, *Organometallics, 6* (1987) 2157.

4 (a) J. R. Shapley, S. I. Richter, M. Tachikawa and J. B. Keister, *J. Organomet. Chem., 94* (1975) C43; (b) M. D. Fryzuk, T. Jones and F. W. B. Einstein, *Organometallics, 3* (1984) 185; M. D. Fryzuk and W. E. Piers, *Polyhedron, 7* (1988) 1001; P. O. Nubel and T. L. Brown, *J. Am. Chem. Soc., 106* (1984) 644, 3474, and refs. therein.

5 (a) K. J. Ahmed, M. H. Chisholm, K. Folting and J. C. Huffman, *J. Am. Chem. Soc., 108* (1986) 989; (b) C. Ting and L. Messerle, *J. Am. Chem. Soc., 109* (1987) 6506; (c) Y. N. Al-Obaidi, M. Green, N. D. White and G. E. Taylor, *J. Chem. Soc., Dalton Trans.*, (1982) 319.

6 D. F. Shriver and M. A. Drezdzon, *The Manipulation of Air-Sensitive Compounds*, 2nd edition, Wiley–Interscience, New York, 1986.

7 R. B. King, Organometallic Syntheses, Vol. 1, Academic Press, New York, 1965, p. 114.

8 (a) T. C. Forschner and A. R. Cutler, *Inorg. Synth., 25* (1989) 231; (b) D. L. Reger and C. Coleman, *J. Organomet. Chem., 131* (1977) 153; (c) E. K. G. Schmidt and C. H. Thiel, *J. Organomet. Chem., 220* (1981) 87.

9 (a) R. B. King and M. B. Bisnette, *J. Organomet. Chem., 2* (1964) 15; (b) A. N. Nesmeyanov, M. I. Rybinskaya, L. v. Rybin, V. S. Kaganovich and P. V. Petrovskii, *J. Organomet. Chem., 31* (1971) 257.

10 T. W. Bodnar and A. R. Cutler, *Organometallics, 4* (1985) 1558.

11 (a) M. L. H. Green and P. L. I. Nagy, *J. Chem. Soc. A.*, (1963) 189, (b) A. Cutler, D. Ehntholt, W. P. Giering, P. Lennon, S. Raghu, A. Rosan, M. Rosenblum, J. Tancrede and D. Wells, *J. Am. Chem. Soc., 98* (1976) 3495; (c) D. E. Laycock, J. Hartgerink and M. C. Baird, *J. Organomet. Chem., 45* (1980) 291.

12 E. J. Crawford, T. W. Bodnar and A. R. Cutler, *J. Am. Chem. Soc., 108* (1986) 6202.

13 P. Treichel, R. L. Shubkin, K. W. Barnett and D. Reichard, *Inorg. Chem., 5* (1966) 1177.

14 (a) R. A. Hoffman and S. Forsen, *Prog. NMR Spectrosc., 1* (1966) 15; (b) J. W. Faller, in F. C. Nachod, and J. J. Zuckerman (eds.), *Determination of Organic Structures by Physical Methods*, Vol. 5, Academic Press, New York, 1973, Chap. 2; (c) M. L. Martin, J. J. Delpuch and G. J. Martin, *Practical NMR Spectroscopy*, Heyden, London, 1980, pp. 315–322; (d) J. Sandstrom, *Dynamic NMR Spectroscopy*, Academic Press, New York, 1982, Chap. 4.

15 (a) F. W. Dahlquist, K. J. Longmuir and R. B. DuVernet, *J. Magn. Reson., 17* (1975) 406; (b) I. D. Campbell, C. M. Dobson, R. G. Ratcliffe and R. J. P. Williams, *J. Magn. Reson., 29* (1978) 397; (c) K. A. Kooistra, J. H. Richards and S. H. Smallcombe, *Org. Magn. Res., 13* (1980) 1.

16 (a) R. B. King and M. B. Bisnette, *J. Organomet. Chem., 7* (1967) 311; (b) R. C. Kerber, W. P. Giering, T. Bauch, P. Waterman and E.-H. Chow, *J. Organomet. Chem., 120* (1976) C31; (c) M. Laing, J. R. Moss and J. Johnson, *J. Chem. Soc., Chem. Commun.*, (1977) 656; (d) P. J. Lennon, A. Rosan, M. Rosenblum, J. Tancrede and P. Waterman, *J. Am. Chem. Soc., 102* (1980) 7033; (e) W. Priester, M. Rosenblum and S. B. Samuels, *Synth. React. Inorg. Met.-Org. Chem., 11* (1981) 525; (f) G. E. Jackson, J. R. Moss and L. G. Scott, *S. Afr. J. Chem., 36* (1983) 69; (g) J. W. Johnson and J. R. Moss, *Polyhedron, 4* (1985) 563.

17 M. Kobayashi and J. D. Wuest, *Organometallics, 8* (1989) 2843.

18 E. Bauch, H. Konowitz, R. C. Kerber and W. P. Giering, *J. Organomet. Chem., 131* (1977) c7.

19 (a) A. Cutler, S. Raghu and M. Rosenblum, *J. Organomet. Chem., 77* (1974) 381; (b) T. C. T. Chang, B. M. Foxman, M. Rosenblum and C. Stockman, *J. Am. Chem. Soc., 103* (1981) 7361; (c) T. C. T. Chang, T. S. Coolbaugh, B. M. Foxman, M. Rosenblum, N. Simms and C. Stockman, *Organometallics, 6* (1987) 2394.

20 IR ν(CO) and ^{1}H NMR δ(Cp) spectral data reflect the charge density on the iron centers of these and related Fp complexes: (a) R. B. King, *Inorg. Chim. Acta, 2* (1968) 454; (b) M. Heberhold and C. R. Jablonski, *Chem. Ber., 102* (1969) 788; M. Heberhold, G. O. Wiedersatz and C. G. Kreiter, *J. Organomet. Chem., 104* (1976) 209; (c) T. W. Bodnar and A. R. Cutler, *J. Am. Chem. Soc., 105* (1983) 5926.

21 Spectral data for the higher homologs [Fp(CH$_2$)$_n$CH=CH$_2$]Fp$^+$ ($n = 3$ and 4) resembles that of **5** ($n = 2$): (a) P. J. Lennon, A. Rosan, M. Rosenblum, J. Tancrede and P. Waterman, *J. Am. Chem. Soc., 102* (1980) 7033.

22 G. S. Bodner, D. E. Smith, W. G. Hatton, P. C. Heah, S. Georgiou, A. L. Rheingold, S. J. Geib, J. P. Hutchinson and J. A. Gladysz, *J. Am. Chem. Soc., 109* (1987) 7688 and refs. therein.

23 Examples (cited as ^{1}H, ^{13}C NMR chemical shifts): (a) Fp=*CH*–CH=CMe$_2$$^+$ (δ 15.96, 316.7), C. P. Casey, W. H. Miles and H. Tukada, *J. Am. Chem. Soc., 107* (1985) 2924; (b) Fp=*CH*Ph$^+$ (δ 16.86, 342.4), M. Brookhart, W. P. Studabaker and M. B. Humphrey, *Organometallics, 8* (1989) 132; (c) Fp=*CH*(c-C$_3$H$_5$)$^+$ (δ 15.47, 365.4), M. Brookhart, W. B. Studabaker and G. R. Husk, *Organometallics, 6* (1987) 1141; (d) Fp=*CH*(OCH$_3$)$^+$ (δ 12.88, 322.3), A. R. Cutler, *J. Am. Chem. Soc., 101* (1979) 604.

24 (a) R. S. Bly, R. K. Bly, M. M. Hossain, L. Lukasy and M. Raja, *J. Am. Chem. Soc., 110* (1988) 7723 and refs. cited.

25 (a) M. Akita, A. Kondoh, T. Kawahara, T. Takagi and Y. Moro-oka, *Organometallics, 7* (1988) 366; (b) M. Akita, T. Kawahara, M. Terada, N. Kakinuma and Y. Moro-oka, *Organometallics, 8* (1989) 687; (c) M. Akita, H. Andoh, O. Mitani, T. Oku and Y. Moro-oka, *J. Mol. Catal., 56* (1989) 107.

26 (a) J. K. P. Ariyaratne, A. M. Bierrum, M. L. H. Green, M. Ishaq, C. K. Prout and M. G. Swanwick, *J. Chem. Soc. A.*, (1969) 1309; (b) E. J. Crawford, C. Lambert, K. P. Menard and A. R. Cutler, *J. Am. Chem. Soc., 107* (1985) 3130.

27 P. Lennon, M. Madhavarao, A. Rosan and M. Rosenblum, *J. Organomet. Chem., 108* (1976) 93.

28 (a) T. W. Bodnar and A. R. Cutler, *J. Organomet. Chem., 213* (1981) C31; (b) A. R. Cutler, P. K. Hanna and J. C. Vites, *Chem. Rev., 88* (1988) 1363; (c) M. Brookhart and W. B. Studabaker, *Chem. Rev., 87* (1987) 411.

29 (a) A. D. Hunter and A. B. Szigety, *Organometallics, 8* (1989) 2670; A. D. Hunter and J. L. McLernon, *Organometallics, 8* (1989) 2679; G. B. Richter-Addo and A. D. Hunter, *Inorg. Chem., 28* (1989) 4065; (b) M. R. J. Piper, G. R. Stephenson, R. J. K. Taylor, C. Breen, J. S. Brooks and G. L. Williams, *J. Chem. Soc., Chem. Commun.*, (1989) 1798 and refs. therein.

30 C. P. Casey, M. S. Konings, M. A. Gohdes and M. W. Meszaros, *Organometallics, 7* (1988) 2103.

31 B. E. Mann, *Annu. Rep. NMR Spectrosc., 12* (1982) 263; K. G. Orrell and V. Sik, *Annu. Rep. NMR Spectrosc., 19* (1987) 79.

32 (a) J. B. Lambert, R. J. Nienhuis and J. W. Keepers, *Angew. Chem., Int. Ed. Engl., 20* (1981) 487; (b) J. K. Sanders and B. K. Hunter, *Modern NMR Spectroscopy*, Oxford University Press, 1987, Chap. 7.

33 (a) R. Benn, A. Rufinska and G. Schroth, *J. Organomet. Chem., 217* (1981) 91; (b) J. K. M. Sanders and J. D. Mersh, *Prog. NMR Spectrosc., 15* (1982) 353.

34 (a) B. E. Mann, *J. Magn. Res., 21* (1976) 17; (b) B. E. Mann, *J. Magn. Res., 25* (1977) 91.

35 (a) T. H. Lawry and K. S. Richardson, *Mechanism and Theory in Organic Chemistry*, 2nd edition, Harper and Row, New York, 1982, p. 403; (b) M. Saunders and H. Siehl, *J. Am. Chem. Soc., 102* (1980) 6868.